Atomic charge exchange between fast helium ions and targets from carbon to bismuth at $\beta = 0.36$

K. Dennis,[1] H. Akimune,[2] G. P. A. Berg,[3] S. Chang,[3] B. Davis,[4] M. Fujiwara,[5]
M. N. Harakeh,[6] J. Jänecke,[1] J. Liu,[3] K. Pham,[1] D.A. Roberts,[1] and E.J. Stephenson[3]
[1] *The University of Michigan, Ann Arbor, Michigan, 48109*
[2] *Department of Physics, Kyoto University, Kyoto 606, Japan*
[3] *Indiana University Cyclotron Facility, Bloomington, Indiana 47408*
[4] *University of Notre Dame, Notre Dame, Indiana 47408*
[5] *Research Center for Nuclear Physics, Osaka University, Osaka 567, Japan*
[6] *Kernfysisch Versneller Instituut, 9747AA Groningen, The Netherlands*
(Received 9 March 1994)

Equilibrium charge-state distributions for singly and doubly ionized ^{3}He ions of energy $E(^3\text{He})$=200 MeV ($\beta = 0.36$) have been measured for atomic targets ranging from carbon to bismuth (Z=6, 14, 28, 40, 50, 67, 73, 83). A magnetic spectrometer was used to simultaneously measure the rate of $^3\text{He}^+$ ions and the current of the incident beam of $^3\text{He}^{2+}$ ions. The ratio of the fraction of ions $Y(^3\text{He}^+)/Y(^3\text{He}^{2+})$ was found to increase from 3×10^{-9} for Z=6 to 2×10^{-7} for Z=83. Very good agreement with the experimental ratios was obtained for calculated ratios based on theoretical stripping (ionization) and capture cross sections. The cross sections are dominated by capture from K orbits only for atoms up to about Z=25. For target atoms with high Z, contributions up to principal quantum numbers n=4 (N orbits) must be included.

PACS number(s): 34.50.Fa, 34.70.+e

I. INTRODUCTION

Collisions between fast moving ions and atoms or molecules in a target lead to the loss (stripping, ionization) and the capture of atomic electrons. The charge composition of the ion beam changes when it penetrates targets thick enough for multiple atomic collisions leading eventually to an equilibrium charge-state distribution. The distribution of charge states as a function of target thickness can be described by a simple system of coupled differential equations. However, these equations contain the charge-changing cross sections for one-electron and multielectron transfer processes. These are very complicated functions which depend on the speed v of the ions, on the atomic number Z_P and charge q_P of the incident ion, and on the atomic number Z_T and the atomic shell $(K, L, M, N, \ldots)$ of the target. For heavy projectiles with $Z \geq 16$ a dependence on whether the target is a gas or a solid was also observed [1]. A comparison of the phenomena for slow [2] and fast [3] ions suggests increased complexity at low projectile energies.

While some of the basic concepts of the description of charge-changing cross sections date back over 60 years and include the work of Niels Bohr [4,5], it was pointed out in 1972 in a review paper by Betz [1] (see also Ref. [6]) that no theory seems to exist which gives a comprehensive description of stripping and capture cross sections. This still appears to be the situation today.

Extensive data exist for protons and other light-ion projectiles. For example, Katayama *et al.* [7–10] have measured equilibrium charge-state distributions as well as electron capture and stripping cross sections for fast He ions at velocities which are 30 to 40 times higher than the Bohr velocity v_0 (see Table I). Detailed comparisons have been made to various theoretical descriptions. The present work presents an extension to even higher velocities of about 50 times the Bohr velocity v_0 [$E(^3\text{He})$=200 MeV]. This corresponds to 36% of the speed of light. It was hoped that the comparison to theoretical and phenomenological predictions will provide further insight into atomic charge-changing processes for fast ions.

A magnetic spectrometer set at $\theta = 0°$ provides a convenient tool [7–10] to detect singly and doubly ionized helium ions. Here, θ is the scattering angle relative to the beam direction. The technique has also been applied by Katayama *et al.* [11] to study the momentum calibration of a magnetic spectrometer. More recently [12] the detection at $\theta = 0°$ of singly ionized $^3\text{He}^+$ in the focal plane together with tritons from the (^{3}He,t) reaction was used as a monitor for the beam energy and the scattering angle which is exactly 0°. The yield of $^3\text{He}^+$ can also be used to monitor on a relative scale, or absolutely after calibration, the beam current and the total charge

TABLE I. Projectile energies E, projectile velocities v, and the ratios $\beta = v/c$ and v/v_0 for the data considered in this work (v_0 = Bohr velocity).

E (MeV)	v (cm/s)	β	v/v_0	Reference
67.9	6.5×10^9	0.22	29.6	Katayama *et al.* [7–10]
99.2	7.8×10^9	0.26	35.9	Katayama *et al.* [7–10]
130.2	8.8×10^9	0.29	40.3	Katayama *et al.* [7–10]
200.0	10.8×10^9	0.36	49.1	Present work
450.0	15.2×10^9	0.51	69.5	Akimune *et al.* [12]

of the incident $^3He^{2+}$ ions in the investigation of (^{3}He,t) reactions near 0° with magnetic spectrometers.

Whereas the present work concentrates exclusively on equilibrium charge-state distributions, several techniques have been developed in recent years [7,9,10,13–15] to determine stripping and capture cross sections individually on gas and solid targets, and also to extract K-capture cross sections by determining the energy loss of the incident ions via precision energy measurements.

Section II describes the experimental techniques, which include the use of a high-resolution magnetic spectrometer, and the results. Theoretical considerations are presented in Sec. III followed by a discussion in Sec. IV.

II. EXPERIMENTAL TECHNIQUES AND RESULTS

The present experiment was performed with a beam of fully ionized $^3He^{2+}$ ions of energy $E(^3He)$=200 MeV from the Indiana University Cyclotron Facility impinging on targets of ^{nat}C, ^{28}Si, ^{56}Ni, ^{90}Zr, ^{A}Sn (A=112, 114, 116, 117, 118, 119, 122, 124), ^{156}Ho, ^{181}Ta, and ^{209}Bi (i.e., Z_T=6, 14, 28, 40, 50, 67, 73, and 83). Some of these targets were also chosen for the investigation of nuclear (^{3}He,t) charge-exchange reactions. The target thicknesses were in the range from 1 to 6 mg/cm^2 which ensures an equilibrium charge-state distribution for singly and doubly ionized ions (e.g., Refs. [7,10]). Both $^3He^+$ and $^3He^{2+}$ ions ("the beam") entered the K600 magnetic spectrometer set at $\theta = 0°$ as shown in Fig. 1. The number of singly ionized $^3He^+$ ions was measured by detecting them individually in the focal plane of the magnetic spectrometer together with tritons from the (^{3}He,t) reaction. Only the trajectory of the $^3He^+$ ions passing through the spectrometer is displayed in Fig. 1. The position spectrum consisting of the $^3He^+$ line at 200 MeV and the triton spectrum was measured with two multiwire drift chambers backed by two thin plastic scintillators. Very good particle identification was achieved using the energy-loss signals from the plastic scintillators. This made it possible to separate ^{3}He and triton events and to establish the wire-chamber efficiencies and the dead time. The corrected number of recorded $^3He^+$ events yielded the total number of events, $Y(^3He^+)$.

The number of fully ionized $^3He^{2+}$ particles was obtained by recording the charge collected in a beam stop located at the inner surface of the first dipole magnet of the magnetic spectrometer. The beam stop is movable along the track as shown in Fig. 1. This allows one to adjust the stop position when the dipole field has to be changed. Since the liner behind the track is also electrically insulated, any charge not reaching the beam stop is recorded here.

The results for the measured ratios $Y(^3He^+)/Y^3He^{2+})$ are shown in Fig. 2. The statistical uncertainties due to the number of observed events $Y(^3He^+)$ are smaller than the data points, but estimated systematic errors of about ±10% are due to uncertainties in the charge integration, the wire-chamber efficiency, and the dead time. The ratio $Y(^3He^+)/Y(^3He^{2+})$ increases continuously with increasing atomic number of the targets from about 3×10^{-9}

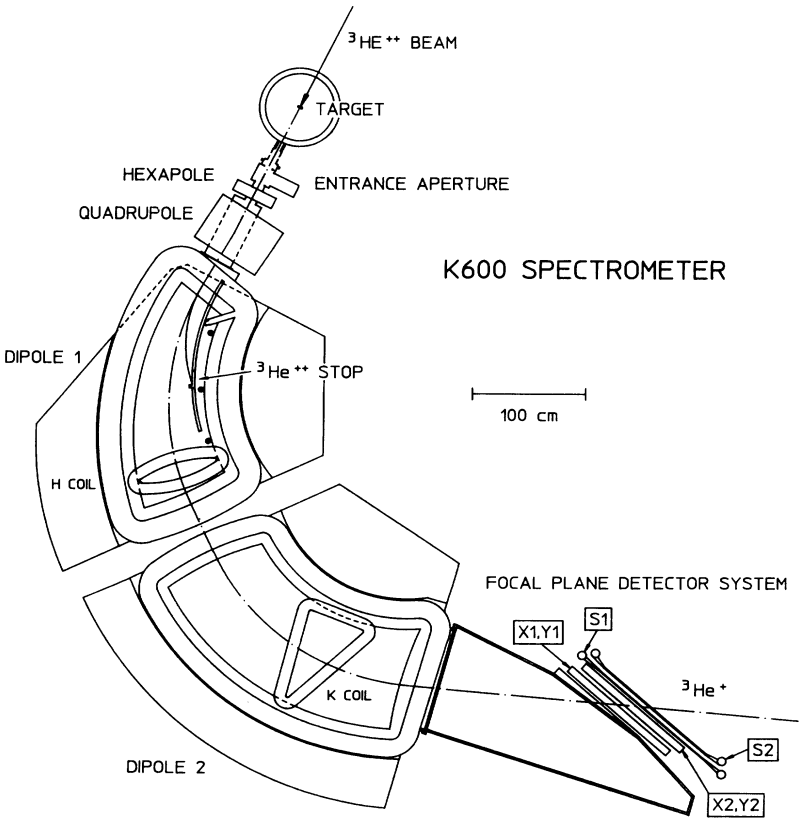

FIG. 1. Schematic diagram of the K600 magnetic spectrometer in the configuration used for the detection of $^3He^+$ and $^3He^{2+}$ ions.

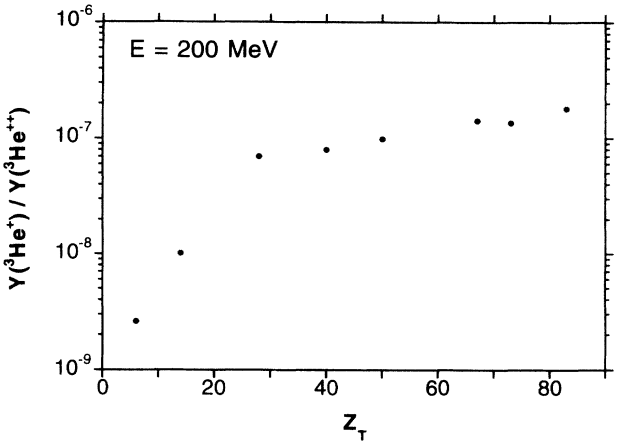

FIG. 2. Experimental equilibrium ratios $Y(^3He^+)/Y(^3He^{2+})$ obtained in the present work at $\beta = 0.36$ [$E(^3He) = 200$ MeV; $v/v_0 = 49$] as a function of the atomic number Z_T for several solid targets.

for Z_T=6 to 2×10^{-7} for Z_T=83. The initial rapid increase over the range from Z_T=6 to Z_T=28 is followed by a much weaker increase for higher Z_T.

No differences within the estimated systematic errors of about ±10% were observed for the isotopes with Z_T=50 from A=112 to 124.

III. THEORETICAL STRIPPING AND CAPTURE CROSS SECTIONS

A. General considerations

Atomic charge exchange between singly and doubly ionized helium ions and target atoms in atomic collisions depends on the speed of the helium projectiles and the atomic charge of the atoms of the target foil. Atomic stripping (ionization) and capture cross sections, σ_{strip} and σ_{cap}, contribute to this phenomenon. Capture may take place from the K, L, M, and higher electron orbits in the target. Both cross sections can be measured independently [7,9,10,13–15]. An equilibrium charge-state distribution is established for high-energy ^{3}He ions in targets with thicknesses greater than typically 50 μg/cm^2 or 2.5×10^{18} atoms/cm^2 for ^{12}C (e.g., Ref. [7,10]).

While neutral atoms must in principle be included in the equilibrium charge-state distribution, their contributions can be neglected at the ion speeds considered in the present experiment. Even the ratios $Y(He^+)/Y(He^{2+})$ are already extremely small (10^{-7} to 10^{-9}).

The fractions of singly and doubly ionized ions, $Y(He^+)$ and $Y(He^{2+})$, must satisfy the system of differential equations [16,1]

$$\frac{dY(He^+)}{dx} = N\{\sigma_{cap}Y(He^{2+}) - \sigma_{strip}Y(He^+)\}, \quad (1)$$

$$\frac{dY(He^{2+})}{dx} = N\{\sigma_{strip}Y(He^+) - \sigma_{cap}Y(He^{2+})\}, \quad (2)$$

with $Y(He^+) + Y(He^{2+}) = 1$. Here, dY/dx describes the variation of Y with target thickness x, and N is the number of target atoms per volume. In equilibrium,

$$\frac{dY(He^+)}{dx} = -\frac{dY(He^{2+})}{dx} = 0, \quad (3)$$

and hence

$$\frac{Y(He^+)}{Y(He^{2+})} = \frac{\sigma_{cap}}{\sigma_{strip}}. \quad (4)$$

The description of the equilibrium charge-state distribution and its dependence on the atomic charge of the target atoms and on the energy of the projectiles requires an understanding of the atomic charge-changing processes.

B. Classical calculations for σ_{strip}

One of the earliest studies of electron stripping (ionization) cross sections in atomic charge exchange was carried out by Bohr [5]. For light ions penetrating through foils of high-Z targets a simple estimate for the stripping cross sections gives

$$\sigma_{strip} \approx \pi a_0^2. \quad (5)$$

Here, a_0 is the Bohr radius. For ion velocities v which are much higher than the Bohr velocity v_0 one can apply the free-collision approximation by neglecting the effect of atomic binding energies. In this approximation Bohr derived

$$\sigma_{strip} = \pi a_0^2 \frac{4Z_T(Z_T+1)}{Z_P^2}\left(\frac{v_0}{v}\right)^2 \quad (6)$$

for low-Z target nuclei. Here, Z_P and Z_T are the atomic numbers of the projectile ion and the target, respectively. However, for targets with intermediate values of Z_T, screening effects due to the tightly bound inner electrons leads to the expression [5]

$$\sigma_{strip} = \pi a_0^2 \frac{Z_T^{2/3}}{Z_P}\left(\frac{v_0}{v}\right). \quad (7)$$

Figure 3 displays the stripping cross sections σ_{strip} based on the theoretical Eqs. (5), (6), and (7) as a function of Z_T for $\beta = 0.36$. The lines for Eqs. (6) and (7) intersect near $Z_T = 10$. Since the two equations have a different dependence on the projectile velocity v and energy E, this intersection shifts slightly from $Z_T \approx 7$ for $E = 68$ MeV to $Z_T \approx 14$ for $E = 450$ MeV.

Detailed calculations for excitation and ionization cross sections of fast one-electron ions, including $^3He^+$, interacting with neutral atoms were also carried out by Gillespie [17]. The calculations are based on the asymptotic (high-energy) Born approximation. Except for a very small higher-order correction term in $\alpha/\beta = v_0/v$ (α is the fine structure constant, $\beta = v/c$, and $v_0 = \alpha c$ is the Bohr velocity), the cross section can be expressed as

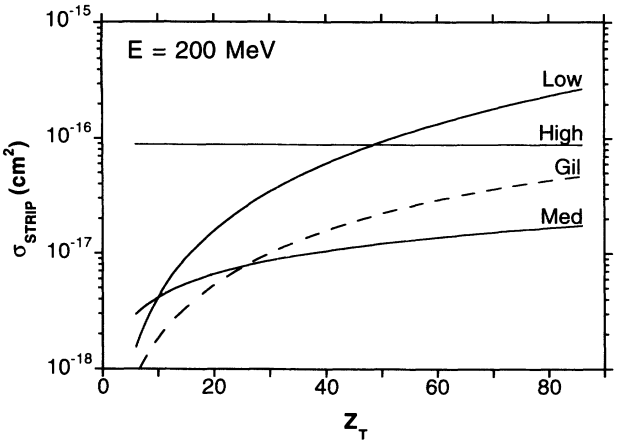

FIG. 3. Calculated atomic stripping (ionization) cross sections for transitions $He^+ \rightarrow He^{2+}$ at $\beta = 0.36$ as a function of the atomic number Z_T of the target atoms (see text). The three solid lines labeled (Low, Med, High) represent the Bohr predictions for presumably low-Z, medium-Z, and high-Z targets [1], respectively. The dashed line (Gil) represents the equation of Gillespie [17].

$$\sigma_{strip} = 8\pi a_0^2 I \left(\frac{v_0}{v}\right)^2. \tag{8}$$

Here, I is the ionization collision strength. Numerical results for the collision strength I were reported [17] only for targets of He, Ne, and Ar, but additional values for $Z_T = 6, 7, 13, 28, 47$, and 79 are included in Ref. [10]. It is interesting to note that the dependence on the projectile velocity v is identical for Eqs. (8) and (6). If one defines the Bohr collision strength as

$$I_B = \frac{Z_T(Z_T+1)}{2Z_P^2}, \tag{9}$$

then Eq. (6) for low-Z atoms can be included in Eq. (8) with $I = I_B$. However, the strengths $I = I_G$ calculated by Gillespie [17,18] are smaller than those of Eq. (9) by factors of $\sim 0.55, \sim 0.35$, and ~ 0.18 for $Z_T = 6, 18$, and 79, respectively. Based on the collision strengths reported by Gillespie [17,18], the purely phenomenological expression for the dependence on Z_T,

$$I_G \approx \frac{1.24}{Z_P^2} Z_T(1 + 0.105 Z_T - 5.4 \times 10^{-4} Z_T^2), \tag{10}$$

reproduces the reported collision strengths very well for $Z_T = 6$ to > 80. For $Z_T = 2$ it overestimates I_G from Ref. [17] by 50%, but it agrees with I_B from Eq. (9).

The cross sections σ_{strip} calculated from this interpolation procedure are included in Fig. 3 as a dashed line. It intersects with the medium-Z line from Eq. (7) near $Z_T = 25$, and the intersection shifts in this case more strongly from $Z_T \approx 14$ for $E = 68$ MeV to $Z_T \approx 45$ for $E = 450$ MeV.

Equations (6), (7), and (8) of Bohr and Gillespie have been applied by Katayama *et al.* [7–10] to the interpretation of experimental stripping cross sections obtained on solid targets of C, Al, Ni, Ag, and Au, and on gas targets of N_2, Ne, and Ar. A good description over the entire range of higher atomic numbers Z_T was found for Eq. (7) by Bohr which accounts for screening effects. This equation was therefore adopted in the present work for all heavier atoms.

Experimental evidence [7–10,14,15] shows that Eq. (7) is apparently not valid for low-Z targets. Here, Bohr's Eq. (6) [5] and Gillespie's Eq. (8) obtained in the asymptotic Born approximation [17] are more appropriate and provide a better description. A close comparison of the data for E=68 to 130 MeV on targets ranging from C to Ar [9,10] with these equations appears to favor Eq. (8), but for the lightest targets of C and N results closer to Eq. (6) were also reported [14].

Adopted theoretical atomic stripping cross sections σ_{strip} were introduced in the present work for the comparison with the data. Equation (8) with Eq. (10) by Gillespie was used for the light target atoms, and Eq. (7) by Bohr for medium-Z target atoms was used for the heavier ones. These equations represent the lower limit of the calculated values for any given value of Z_T as can be seen from Fig. 3.

C. Classical calculations for σ_{cap}

One of the earliest works to describe capture cross sections is that of Oppenheimer-Brinkmann-Kramer (OBK) [19–21]. They derived the asymptotic expression

$$\sigma_{OBK} = \pi a_0^2 \frac{2^{18}}{5} Z_P^5 Z_T^5 \left(\frac{v_0}{v}\right)^{12} \tag{11}$$

in first-order Born approximation. In second- and third-order Born approximation [21] one obtains

$$\sigma_{B2} = \sigma_{OBK}\left\{0.295 + \frac{5\pi}{2^{11}} \frac{1}{Z_P + Z_T}\left(\frac{v_0}{v}\right)\right\}. \tag{12}$$

A generalization of the OBK method including arbitrary external and internal screening corrections for atomic capture cross sections has been derived by Nikolaev [22]. One-electron hydrogenlike wave functions were employed. The Nikolaev capture cross section [see Eq. (10) of Ref. [22]] consists of a superposition of contributions from capture of an electron into a state with principal quantum number n in the projectile from the K, L, and higher shells with principal quantum numbers n_i in the target. It can be written as

$$\sigma_{cap} = \pi a_0^2 \frac{2^8}{5}\left(\frac{v_0}{v}\right)^2 \times \sum_{K,L,M,\ldots} N_i n^2 \gamma_i^5 \eta_i^5 \frac{(1+\delta_i)^{5/2}}{(1+\delta_i\gamma_i)^3} \Phi_4(\delta_i\gamma_i). \tag{13}$$

Here, N_i is the number of electrons in orbits with principal quantum number n_i. For the heaviest atoms capture from orbits up to principal quantum numbers $n_i = 4$ and $n_i = 5$ (N and O orbits) were considered. The quantities γ_i and η_i entering into Eq. (13) depend on the speed u of the electrons in the $K, L, M, \ldots$ orbits of

the target atom derived in the one-electron approximation from $\epsilon_i = \mu u^2/2$ with atomic binding energies ϵ_i (μ = electron mass). The ratio $V \equiv v/u$, where v is the projectile speed, enters into Eq. (13) as an important parameter. The quantity δ_i is related to the usually employed screening parameter [see Ref. [22] for further definitions of the various quantities in Eq. (13)]. In using the expressions given by Nikolaev [22] to calculate the capture cross section, the atomic binding energies were taken from Ref. [23], and the screening corrections and effective charges $Z_T^* = Z_T - s$ were calculated by evaluating the Slater rules [24] for each electronic subshell. A small phenomenological correction function introduced by Nikolaev was included in the calculations and will be discussed below.

Equation (13) for the capture cross sections [22] was found by Katayama *et al.* [9,10] to reproduce quite well measured capture cross sections $^3He^{2+} \rightarrow {}^3He^+$ for targets of Al, Ni, Ag, and Au, and bombarding energies of 68, 99, and 130 MeV, whereas the results based on the first- and second-order OBK approximation [19–21] of Eqs. (11) and (12) were found to strongly overestimate the experimental data, particularly for higher values of Z_T. The Nikolaev equation was therefore adopted in the present work to represent the capture cross sections σ_{cap} at the bombarding energy of 200 MeV.

Figure 4 displays for E=200 MeV ($\beta = 0.36$) the quantity σ_{cap} based on the OBK Eqs. (11) and (12) as dotted lines. Results from the Nikolaev Eq. (13) are shown as heavy solid lines. The individual contributions from the capture from the K, L, M, N, and O shells with the principal quantum numbers $n_i = 1$ to 5 are also shown.

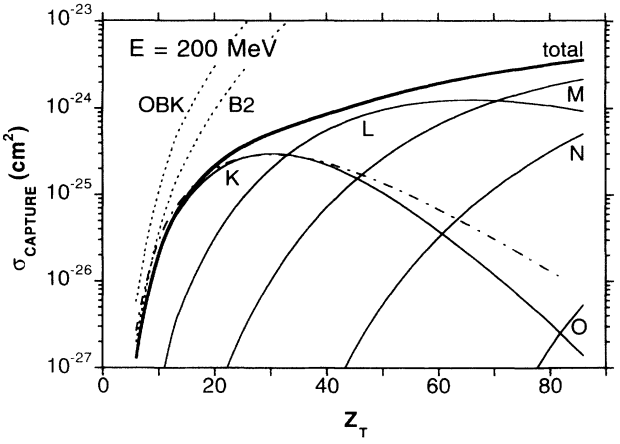

FIG. 4. Calculated atomic electron-capture cross sections for transitions $He^{2+} \rightarrow He^+$ at $\beta = 0.36$ as a function of the atomic number Z_T of the target atoms (see text). The calculated cross sections from the Nikolaev equation [22] (solid lines) represent a superposition of contributions for electron capture from the atomic shells $K \rightarrow O$. Predictions from the first- and second-order OBK approximation (see text) are shown as dotted curves, and the predictions for electron capture from the K orbits based on a relativistic equation (see text) is shown as a dash-dotted line.

D. Relativistic calculations

Anholt and Eichler [25] have calculated the cross sections for electron capture by relativistic projectiles in the eikonal approximation. In the formalism developed they were able to evaluate the cross section for electron capture into the K shell of the projectile from the K and L shells of the target by a numerical integration of a two-dimensional integral. However, in case the target and projectile charges are small, i.e., αZ_T and αZ_P are much less than unity (α is the fine structure constant), the integral can be expanded to first order in αZ_T to yield an approximate formula [Eq. (4) in Ref. [25]] for the $1s_{1/2}$-$1s_{1/2}$ (K-K) cross section. By neglecting the phase distortion of the final-state wave function of the transferred electron it could be shown that this formula reduces to the relativistic OBK approximation. A more detailed description of the theoretical framework in which the above equation has been derived in the eikonal approximation can be found in Refs. [26,27].

We have used this formula to evaluate the K-K cross section for ^3He projectiles as function of Z_T at bombarding energies of 200 and 450 MeV. In this calculation, we have utilized the experimental binding energies for the 1s electrons in the target nuclei [23]. Adopted effective charges $Z_T^* = Z_T - s$ with $s = 0.3$ were assumed for the $1s_{1/2}$ orbitals to account for the partial shielding by inner-shell electrons. The results are included in Fig. 4 as a dash-dotted curve.

IV. DISCUSSION

Figure 5 displays the experimental data for the ratios $Y(He^+)/Y(He^{2+})$ together with calculated ratios $\sigma_{cap}/\sigma_{strip}$ as a function of Z_T. The results from the

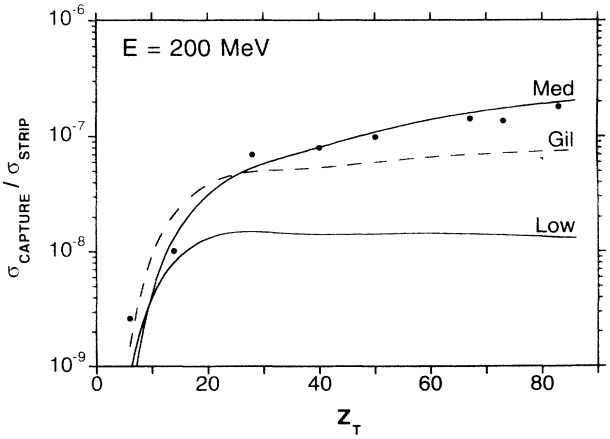

FIG. 5. Experimental equilibrium ratios $Y(^3He^+)/Y(^3He^{2+})$ obtained in the present work at $\beta = 0.36$ as a function of the atomic number Z_T for several solid targets and comparison to calculated ratios $\sigma_{cap}/\sigma_{strip}$ based on the Nikolaev equation [22] for σ_{cap} and three equations [1, 13] for σ_{strip} (Low = Bohr low-Z; Med = Bohr medium-Z; Gil = Gillespie).

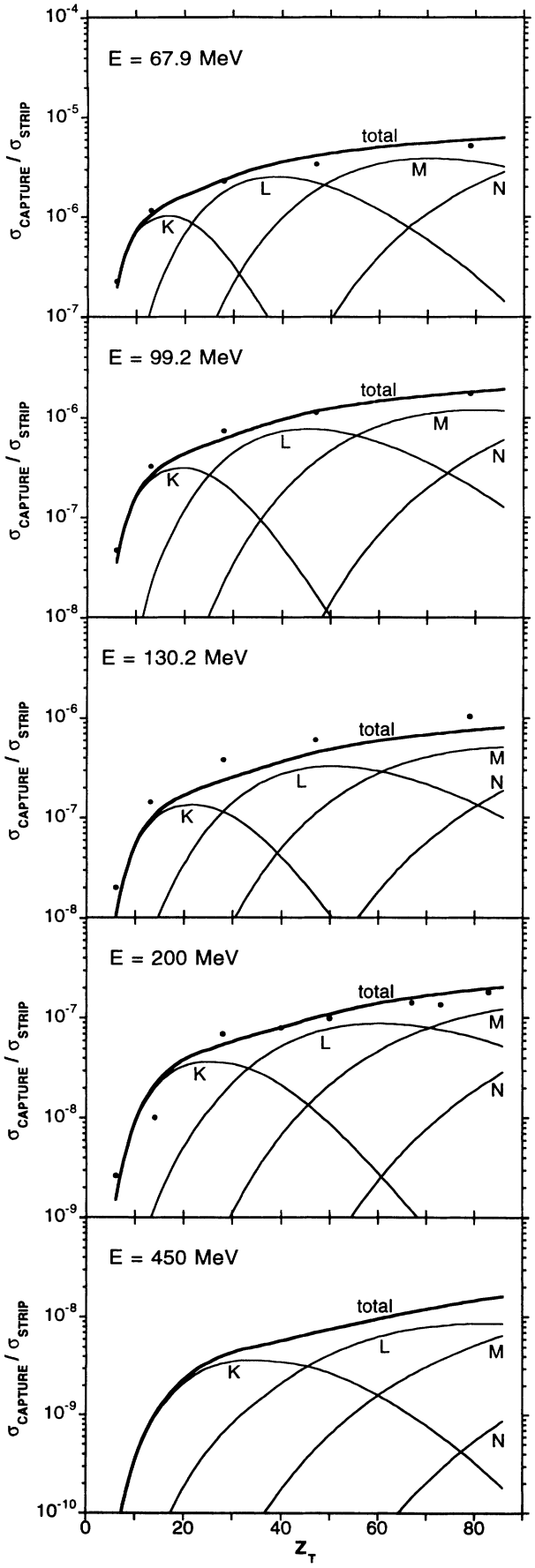

Nikolaev equation (13) were used to describe the capture cross sections σ_{cap}. Three expressions for the stripping cross sections σ_{strip} were employed. These are Eqs. (6), (7), and (8) with (10) for the low-Z and medium-Z approximations of Bohr [5] and the expression of Gillespie [17]. The respective curves in Fig. 5 are labeled (Low), (Med), and (Gil). As expected, curve (Med), i.e. the combination of the Nikolaev equation for σ_{cap} with the medium-Z expression of Bohr for σ_{strip}, describes the data for the heavier atoms quite well.

The situation for the measured ratios $Y(\mathrm{He}^{+})/Y(\mathrm{He}^{2+})$ for $Z_T = 6$ and 14 is not quite clear. The experimental values are slightly high or low compared to curve (Gil) which was calculated from the adopted cross sections as outlined in Sec. III C. Oxygen and carbon surface contaminations of the target are known to have an influence on measured stripping cross sections [15]. Oxygen surface contaminations of the ^{28}Si target were present and could indeed lower the measured value. However, the estimated thickness was not sufficient for such an explanation.

Figure 6 displays the experimental and calculated ratios $Y(^3\mathrm{He}^{+})/Y(^3\mathrm{He}^{2+})$ and $\sigma_{cap}/\sigma_{strip}$, respectively, for energies of 67.9, 99.2, 130.2, 200, and 450 MeV. The respective velocities are listed in Table I. The experimental ratios are from the work of Katayama *et al.* [7–10] and from the present work. Calculated ratios for 450 MeV are included because extensive (^{3}He,t) work together with the measurement of $^3\mathrm{He}^{+}$ yields is presently in progress at the Research Center for Nuclear Physics, Osaka University [28]. The calculated cross sections are from the capture expression of Nikolaev [22], Eq. (13), divided by the adopted stripping cross sections of Gillespie [17] and Bohr [5], Eqs. (8) and (7), respectively. Furthermore, as in Fig. 4, the cross sections σ_{cap} are decomposed into the contributions from the various atomic shells. The overall agreement between the experimentally determined ratios and the calculated ratios $\sigma_{cap}/\sigma_{strip}$ is remarkably good except for the 130-MeV data, which are slightly high possibly suggesting a normalization problem in the experimental data, and the low ^{28}Si point for 200 MeV which was mentioned above. A preliminary analysis of the ratio $Y(\mathrm{He}^{+})/Y(\mathrm{He}^{2+})$ measured recently [28] for ^{58}Ni ($Z_T = 28$) at $E(^3\mathrm{He}) = 450$ MeV near the maximum of the K-shell capture cross section is also in very good agreement within a few percent of the calculated value of 3×10^{-9}.

Figures 4 and 6 show the decomposition of the combined capture cross section or cross section ratios into

FIG. 6. Experimental and calculated equilibrium ratios $Y(^3\mathrm{He}^{+})/Y(^3\mathrm{He}^{2+})$ for $E(^3\mathrm{He}) = 68$, 99, 130, 200, and 450 MeV as a function of the atomic number Z_T of the target atoms. The absolute and relative ion velocities are listed in Table I. The experimental ratios are from the work of Katayama *et al.* [7–10] and from the present work. The calculated ratios of the atomic stripping and capture cross sections (solid lines) were obtained from the adopted cross section expressions (see text). They are decomposed into the contributions with capture from the K, L, M, and higher atomic orbits of the targets.

the contributions of capture from the $K, L, M, \ldots$ shells in the target atoms. This explains the initial pronounced increase as a function of Z_T of σ_{cap} and $\sigma_{cap}/\sigma_{strip}$, respectively. It is due to electron capture from the K orbit of the target atom which dominates for small Z_T and displays a pronounced maximum. The initial strong increase is followed by a subsequent continued slow increase due to the superposition of electron capture from the L and higher shells. The data demonstrate the need for including atomic orbits up to $n_i = 4$ (N orbit) to describe the data for large Z_T. Orbits with $n_i = 5$ (O orbits) contribute only $\sim 1\%$ at $Z_T = 100$ for E=200 MeV, slightly more at lower bombarding energy, and can therefore be neglected.

The calculated maxima in σ_{cap} for the K and L orbits as displayed in Fig. 4 for $E(^3\mathrm{He}) = 200$ MeV occur when in the Nikolaev equation (13) the ratio $V \equiv v/u \approx 1.84$ (K orbit) or ≈ 1.97 (L orbit); (v = projectile speed; u = classical electron speed in the atomic orbit of the target). This result is not obvious and contradicts the classical picture that the velocity of the projectile should match the velocities of the electron in the initial and final orbits, hence $V \approx 1$.

Considering Eq. (13) one finds that the capture cross sections σ_{cap} depend on v and u individually and not only on the ratio V. Therefore one has to consider two cases.

The dependence on v for fixed u (dependence on E for fixed Z_T) has a maximum at $V = \sqrt{2/3} = 0.82$ (without screening; independent of Z_T) and $V \approx 0.85$ (with screening). These values are close to the classical estimate $V \approx 1$.

The dependence on u for fixed v (dependence on Z_T for fixed E) has a maximum at $V = \sqrt{3} = 1.73$ (without screening; independent of E; for K and L orbits) and $V \approx 1.84$ or 1.97 (with screening; weak dependence on E; for K or L orbits). The departure of V for maximum σ_{cap} as shown in Fig. 4 from the classical estimate $V \approx 1$ is due to the fact that σ_{cap} depends not only on the relative velocities $V \equiv v/u$ but also on other factors including the size of the atomic orbits.

It must be noted that in using the Nikolaev equation (13) for calculating capture cross sections σ_{cap}, the result was multiplied by the one-parameter phenomenological correction function

$$R_0(t) = \frac{0.3}{(t^{-8} + t)^{0.2}} \tag{14}$$

with

$$t = \frac{7}{9}\frac{v}{v_0\sqrt{b}} \tag{15}$$

before comparison with the experimental results. Here, v is again the projectile velocity, v_0 is the Bohr velocity, and $b = Z_T^*/n_i$ is given by the effective charge $Z_T^* = Z_T - s$ and the principal quantum number n_i. This semiempirical function of Eq. (14) was constructed by Nikolaev [22] to ensure agreement with experimental capture cross sections for protons (hydrogen) of energies 20 keV to 13 MeV in gases from hydrogen to krypton. Yet, interestingly, as shown, the semiempirical correction appears to be still valid for helium ions of much higher speed and for even the heaviest targets. At the bombarding energy of $E(^3\mathrm{He}) = 200$ MeV, the correction $R_0(t)$ ranges from about 0.15 to 0.20. The quantity $R_0(t)$ does not change drastically with the effective charge of the target and the speed of the projectile v, and it increases only slightly at lower projectile energies. A possible connection of this factor with the presence of multistep processes has been suggested [29], but the origin of the correction function becomes less clear when it is recognized that the relativistic calculations (see below) do not require such a correction.

The relativistic calculations [25] for pickup from K orbits as described in Sec. III D are displayed in Fig. 4 as a dash-dotted line.[1] Since the eikonal approximation [30] requires the projectile velocity to exceed the orbital velocities of the electron in the initial and final states (i.e., target and projectile), a sufficient condition is $v/u \geq 2$. This limits the applicability to the region of low Z_T below the maximum. Furthermore, as mentioned earlier, the analytical expansion of the integral obtained in the eikonal approximation requires $\alpha Z_T \ll 1$ and $\alpha Z_P \ll 1$. As expected, the relativistic calculations for capture from the K orbit agree well with the Nikolaev calculations below the maximum but begin to deviate at higher Z_T.

It has been mentioned in Sec. II that data were obtained for eight Sn isotopes with mass numbers A ranging from 112 to 124. The nuclear radius increases over this mass range by about 3.5%. No isotope shift could be observed for the atomic cross sections. The cross section ratios increase by $(0.4 \pm 0.6)\%$ per mass number which is compatible with zero. This result confirms the atomic nature of the effects.

In conclusion, ratios of the fractions of singly and doubly ionized helium ions, $Y(^3\mathrm{He}^+)/Y(^3\mathrm{He}^{2+})$, were measured at 200 MeV which corresponds to a projectile speed of $\beta = 0.36$. These data and data obtained by Katayama *et al.* [7–10] at lower bombarding energies were compared to theoretical ratios of atomic electron capture to stripping cross sections. Surprisingly good agreement has been achieved.

Atomic capture cross sections were described by the equation derived by Nikolaev [22] which represents a generalization of the OBK method including arbitrary external and internal screening corrections. One-electron hydrogenlike wave functions are used in these calculations, and the calculated cross sections represent the superposition of the contributions from electron capture from the $K, L, M, \ldots$ orbits in the target atoms. Contributions up to principal quantum number $n_i = 4$ (N orbits) must be included for the heaviest target atoms. A semiempir-

[1] It should be noted that in trying to reproduce the results of Ref. [25] obtained with the relativistic formula described in Sec. III D for Ne ions of energy 1050 MeV/A on a number of targets (columns 3 and 7, Table I of Ref. [25]), we found values that were larger by a factor of 1.5 than reported by Anholt and Eichler [25]. The results shown in Fig. 4 have not been reduced by this factor.

ical correction term introduced by Nikolaev, while very successful, is not understood.

Stripping cross sections for atoms with small atomic numbers Z_T were described with the equation of Gillespie [17] which is based on the asymptotic (high-energy) Born approximation. However, this equation overestimates the cross sections for higher atomic numbers ($Z_T > 29$ for E=200 MeV) apparently due to the neglect of screening corrections. Here, the expression derived by Bohr [5] for medium-Z atoms which includes screening effects due to the tightly bound inner electrons was found to give good agreement.

ACKNOWLEDGMENTS

The authors acknowledge helpful discussions with Professors I. Katayama and K. T. Hecht and the important support by the technical staff of the IUCF, in particular C. C. Foster and W. Lozowski. Computational assistance was provided by D. Nykamp. This research was supported in part by the National Science Foundation, Grant Nos. PHY-9208468 (UM, Ann Arbor) and PHY-9015057 (IUCF). The NATO Travel Grant No. 90-0219 provided by the Scientific Affairs Division, North Atlantic Treaty Organization, is gratefully acknowledged.

[1] H. D. Betz, Rev. Mod. Phys. **44**, 465 (1972).
[2] T. R. Dillingham, J. R. Macdonald, and P. Richard, Phys. Rev. A **24**, 1237 (1981) and references therein.
[3] R. D. Rivarola, G. R. Deco, and J. M. Maidagan, Nucl. Instrum. Methods B **10/11**, 222 (1985) and references therein.
[4] L. H. Thomas, Proc. R. Soc. London Ser. A **114**, 561 (1927).
[5] N. Bohr, K. Dan. Vidensk. Selsk. Mat.-Fys. Medd. **18**. No. 8 (1948).
[6] A. B. Wittkower and H. D. Betz, At. Data **5**, 113 (1973).
[7] I. Katayama, G. P. A. Berg, W. Hürlimann, S. A. Martin, J. Meissburger, W. Oelert, M. Rogge, J. G. M. Römer, J. L. Tain, and B. Styczen, Phys. Lett. **92A**, 385 (1982).
[8] I. Katayama, G. P. A. Berg, W. Hürlimann, S. A. Martin, J. Meissburger, W. Oelert, M. Rogge, J. G. M. Römer, J. L. Tain, B. Styczen, and G. Gaul, Phys. Rev. A **27**, 2738 (1983).
[9] I. Katayama, G. P. A. Berg, W. Hürlimann, S. A. Martin, J. Meissenburger, W. Oelert, M. Rogge, J. G. M. Römer, J. L. Tain, L. Zemlo, and G. Gaul, J. Phys. B **17**, L23 (1984).
[10] I. Katayama, G. P. A. Berg, S. A. Martin, J. Meissenburger, W. Oelert, A. Retz, M. Rogge, J. G. M. Römer, G. Gaul, H. Hasai, J. L. Tain, and L. Zemlo, Z. Phys. D **3**, 73 (1986).
[11] I. Katayama, S. Morinobu, Y. Fujita, M. Fujiwara, T. Yamazaki, and H. Ikegami, Nucl. Instrum. Methods **171**, 195 (1980).
[12] H. Akimune, I. Daito, Y. Fujita, M. Fujiwara, M. B. Greenfield, M. N. Harakeh, T. Inomata, J. Jänecke, K. Katori, S. Nakayama, H. Sakai, Y. Sakemi, M. Tanaka, and M. Yosoi, Phys. Lett. B **323**, 107 (1994).
[13] H. Ogawa, I. Katayama, Y. Haruyama, T. Noro, H. Ikegami, F. Fukuzawa, K. Yoshida, A. Aoki, and I. Sugai, Nucl. Instrum. Methods A **262**, 23 (1987).
[14] Y. Haruyama, I. Katayama, H. Ogawa, T. Noro, H. Ikegami, F. Fukuzawa, K. Yoshida, A. Aoki, and I. Sugai, Nucl. Instrum. Methods B **33**, 220 (1988).
[15] Y. Haruyama, H. Ogawa, I. Katayama, T. Noro, H. Ikegami, F. Fukuzawa, K. Yoshida, M. Tosaki, A. Aoki, and I. Sugai, Nucl. Instrum. Methods B **48**, 130 (1990).
[16] S. A. Allison, Rev. Mod. Phys. **30**, 4 (1958).
[17] G. H. Gillespie, Phys. Rev. A **18**, 1967 (1978); A **26**, 2421 (1982).
[18] G. H. Gillespie, private communication quoted in Ref. [10].
[19] J. R. Oppenheimer, Phys. Rev. **31**, 349 (1928); H. C. Brinkmann and H. A. Kramers, Proc. K. Ned. Akad. Wet. **33**, 973 (1930).
[20] R. Shakeshaft and L. Spruch, Rev. Mod. Phys. **51**, 369 (1979).
[21] R. Shakeshaft, Phys. Rev. A **17**, 1011 (1978).
[22] V. S. Nikolaev, Zh. Eksp. Teor. Fiz. **51**, 1263 (1966) [Sov. Phys. JETP **24**, 847 (1967)].
[23] *Table of Isotopes*, 7th ed., edited by C. M. Lederer and V. S. Shirley (Wiley, New York, 1978), Appendix III.
[24] J. C. Slater, Phys. Rev. **36**, 57 (1930).
[25] R. Anholt and J. Eichler, Phys. Rev. A **31**, 3505 (1985).
[26] J. Eichler, Phys. Rev. **A 32**, 112 (1985).
[27] J. Eichler, Nucl. Instrum. Methods B **23**, 23 (1987).
[28] M. Fujiwara *et al.* (unpublished).
[29] I. Katayama, private communication.
[30] J. Eichler and H. Narumi, Z. Phys. A **295**, 209 (1980).